JOURNAL OF THERMOPHYSICS AND HEAT TRANSFER
Vol. 22, No. 1, January–March 2008

Technical Notes

TECHNICAL NOTES are short manuscripts describing new developments or important results of a preliminary nature. These Notes should not exceed 2500 words (where a figure or table counts as 200 words). Following informal review by the Editors, they may be published within a few months of the date of receipt. Style requirements are the same as for regular contributions (see inside back cover).

Modeling for the Transient Radiative Properties of Alumina Particles with Phase Transition

Shi-Kui Dong,* Jia-Yu Li,† Zhi-Hong He,* and He-Ping Tan‡
Harbin Institute of Technology,
150001 Harbin, People's Republic of China

DOI: 10.2514/1.32202

Nomenclature

F_x	=	volume fraction of the x component in the whole particle
f_α	=	portion of the α phase during the transition from the γ phase to the α phase
I_λ	=	particle's spectral radiance
k	=	imaginary part of the complex refractive index (absorption coefficient)
m	=	complex refractive index of the mixture
M_x	=	portion of the x phase in the whole particle
m_x	=	complex refractive index of the x component
n	=	real part of the complex refractive index (refractive index)
$Q_{\text{abs},\lambda}$	=	absorption factor of the particle
r	=	radius of the particle
r_L	=	equivalent radius of the liquid fraction of the particle
r_s	=	equivalent radius of the solid fraction of the particle
r_s^*	=	relative crystallization-front radius
T_m	=	equilibrium melting temperature
T_s	=	crystallization-front temperature
V_x	=	volume of the x component
Δt	=	time step
ε_λ	=	spectral emissivity of the particle
ε_x	=	dielectric constant of the x component
ε	=	dielectric constant of the mixture
ε_d	=	dielectric constant of the host medium

Subscripts

L	=	liquid phase
α	=	alpha phase
γ	=	gamma phase

Received 17 May 2007; revision received 27 June 2007; accepted for publication 4 July 2007.

*Associate Professor, School of Energy Science and Engineering, 92 West DaZhi Street.
†Graduate Student, School of Energy Science and Engineering, 92 West DaZhi Street.
‡Professor, School of Energy Science and Engineering, 92 West DaZhi Street; tanheping77@yahoo.com.cn.

I. Introduction

PARTICLE radiation is an important issue for heat transfer or spectral radiation signal transmission in high-temperature a combustion system such as a boiler furnace, a rocket engine combustion chamber, and an exhaust plume [1–4]. A solid aluminized rocket motor produces large amounts of alumina particles, which are the main cause of the plume's radiative properties. When exposed to the cold environment, the cooling alumina particles will crystallize and pass through different phase states, and so the radiative properties of the alumina particle's various phase states should be considered accurately during crystallization. Plastinin et al. [3] studied the spectral radiance of rapidly cooling (3×10^3 K/s) melted alumina particles and indicated that the time dependence of spectral radiative properties is obvious during their crystallization processes and that the effects of equilibrium and nonequilibrium crystallization processes are important in the simulation of the solid propellant motor plume's radiative properties. Rodionov et al. [4] simulated alumina particles' phase transitions and undercooling phenomena in the plume flowfields. Gosse et al. [5] indicated that the morphological and structural properties of Al_2O_3 particles are the important parameters to the plume thermal radiation. Burt and Boyd [6] presented that the crystallization process of the particles becomes more important within the plume near-field region. In literature [7], it is concluded that the particles' morphology and nature (e.g., phase) directly impact their optical properties and indirectly impact their particle-size measurement.

Because of important effects of the phase transition of alumina particles on radiation characteristics of solid propellant motor exhaust, this Note analyzes the experiment results of the Al_2O_3 particles' phase transition and simulates the time dependence of the volume fraction of the Al_2O_3 particles, with each phase based on the kinetic equation of the Al_2O_3 particles' crystallization process (liquid—γ phase—α phase). Two kinds of models are built up based on two possible solidification modes, including the multilayered sphere model and the effective-medium sphere model. In the multilayered sphere model, the light-scattering subroutine for n-layered spheres [8] is used to calculate absorption and scattering parameters of Al_2O_3 particles. In the effective-medium sphere model, several appropriate mixing rules of effective-medium theory (EMT), such as the volume-average dielectric constant (VADC), the volume-average refractive index (VARI), the Bruggeman mixing rule, and the Maxwell–Garnett (M–G) mixing rule, are chosen to calculate the effective optical constants of Al_2O_3 particles, and the absorption and scattering parameters are calculated by Mie theory.

II. Phase-Transformation Kinetics of Alumina Particles

In the solidification of the liquid alumina particle in rocket exhaust plume, it is most likely to evolve into the gamma γ phase. Then, if there is sufficient time, it may progress through other phases (delta and theta) until it finally transforms into the stable alpha α phase [9]. In this Note, we simplified the solidification process, and only the transformation process of the three phase states (liquid, gamma, and alpha) is studied.

A. Kinetics Process of Liquid-to-Gamma-Phase Transition

As the temperature decreases in the plume, the Al_2O_3 particles experience the liquid–solid transition. It is a nonequilibrium process, and the recession of the crystallization front is described by the equation [3]

$$r_s(\mathrm{d}r_s^*/\mathrm{d}t) = -a^*(T_m - T_s)^{1.8} \tag{1}$$

where t is time, $a^* = 0.64 \times 10^{-6}$ m/s × K$^{1.8}$, T_m is the equilibrium melting temperature taken as $T_m = 2327$ K, T_s is the crystallization-front temperature , $T_s \cong 2273$ K [10], r_s is the equivalent radius of the solid fraction of the particles, and r_s^* is the relative crystallization-front radius. The particle in the liquid state is denoted by $r_s^* = 1$, and $r_s^* = 0$ corresponds to the solid state. If the particle is in the transitional states, $0 < r_s^* < 1$.

B. Kinetics Process of Gamma-to-Alpha-Phase Transition

The process of transition between the γ phase and α phase begins as soon as the γ phase has appeared. To determine the portion of α phase f_α during the transition from the γ phase to the α phase, the following equation was applied [3]:

$$\mathrm{d}f_\alpha/\mathrm{d}t = a_\alpha \cdot \exp(-b_\alpha/T) \tag{2}$$

where a_α and b_α are empirical coefficients, $b_\alpha = 58,368$ K, and $a_\alpha = 1.5 \times 10^{12}$ 1/s. The particle's temperature T is constant during the transition process: $T = 2310$ K [11].

From literature [3,4], the portion of the γ phase (M_γ) and α phase (M_α) in the whole particle would be defined by the following equations:

$$M_\gamma = (1 - M_L)(1 - f_\alpha), \qquad M_\alpha = (1 - M_L)f_\alpha \tag{3}$$

$$M_\gamma = (1 - (r_s^*)^3)(1 - f_\alpha), \qquad M_\alpha = (1 - (r_s^*)^3)f_\alpha \tag{4}$$

C. Volume Fraction of Each Phase in the Process of Phase Transition

In the process of liquid–solid transition, the function between the radius of solid fraction r_s and the radius r of the particle is deduced:

$$r_s = \sqrt[3]{r^3 - r_L^3} \tag{5}$$

where r_L is the equivalent radius of the liquid fraction of the particle.

Based on Eqs. (3) and (4), the expression for the relative crystallization-front radius r_s^* can be deduced:

$$r_s^* = \frac{r_L}{r} \tag{6}$$

This expression satisfies the condition for r_s^*. By substituting Eqs. (5) and (6) into Eq. (1), the function of r_L is deduced:

$$\sqrt[3]{1 - \left(\frac{r_L}{r}\right)^3}(\mathrm{d}r_L/\mathrm{d}t) = -a^*(T_m - T_s)^{1.8} \tag{7}$$

Solving this equation with the fourth-order Runge–Kutta method, the radius of liquid Al_2O_3 at each time point can be achieved, and then the volume of liquid Al_2O_3 is obtained. The time step is a fixed step ($\Delta t = 0.002$ s).

During the phase transition, the liquid phase is first transformed to a metastable γ phase. Basing on the kinetic equation for a first-order reaction, the transition from γ to α phase happens at the same time. The volume of new γ-phase Al_2O_3 in an arbitrary time step can be expressed as

$$\Delta V_\gamma(t) = -[V_L(t - \Delta t) - V_L(t)] \tag{8}$$

The volume of a new α-phase Al_2O_3 in the same time step is expressed as

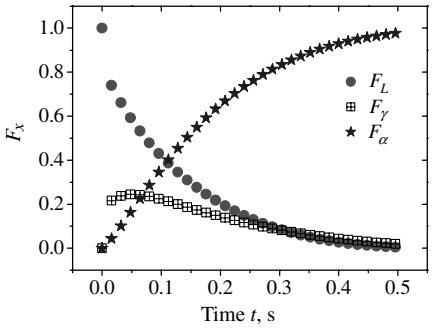

Fig. 1 Volume fractions of liquid, gamma, and alpha alumina.

$$\Delta V_\alpha(t) = V_\gamma(t - \Delta t) \cdot f_\alpha(\Delta t) \tag{9}$$

and so the volume of γ phase at time t is deduced

$$V_\gamma(t) = V_\gamma(t - \Delta t) + \Delta V_\gamma(t) - \Delta V_\alpha(t) \tag{10}$$

and the volume of α phase at time t is deduced:

$$V_\alpha(t) = V_\alpha(t - \Delta t) + \Delta V_\alpha(t) \tag{11}$$

When the time dependence of the volume for three phase states is known, the volume fraction for these phase states (F_L, F_γ, and F_α) at every time point can be calculated; results are shown in Fig. 1.

III. Time-Dependence Modeling of Alumina Particles' Spectral Radiance in Phase Transitions

Suppose that the Al_2O_3 particle is a diffuse object, then the function for the particle's spectral radiance can be deduced:

$$I_\lambda = \frac{\varepsilon_\lambda E_{b\lambda}}{\pi} = \varepsilon_\lambda \frac{c_1\lambda^{-5}}{\exp[c_2/(\lambda T)] - 1} \cdot \frac{1}{\pi} \tag{12}$$

The spectral emissivity ε_λ of a big spherical particle is equal to its absorption factor $Q_{\mathrm{abs},\lambda}$, which can be calculated by Mie theory:

$$\varepsilon_\lambda = Q_{\mathrm{abs},\lambda} \tag{13}$$

The solidification process of an Al_2O_3 particle is very complex. Two possible solidification modes are assumed in this Note, which are layer-by-layer solidification and normal solidification. On the basis of two possible solidification modes, two kinds of models are built up, described next.

A. Multilayered Sphere Model

In this model, the solid zone moves from the surface to the core in melted Al_2O_3 particles under the cold environment, and so the solidification is assumed to be in layer-by-layer mode. We assume that the geometry of this model is a core of liquid Al_2O_3 sphere surrounded by two concentric spherical layers that are in α and γ phases from the outside to inside. The schematic diagram of this model is shown in Fig. 2. As the phase transitions go on, the volume of the three components changes based on Eqs. (2) and (7–11). The absorption and scattering factors of the three-layered sphere are calculated by use of the light-scattering subroutine for n-layered spheres [8], and the temperature of the Al_2O_3 particle stays constant ($T = 2310$ K) during this stage [11]. Then the spectral radiance during the particle's phase transition is calculated by a combination of Eqs. (12) and (13).

B. Effective-Medium Sphere Model

In the effective-medium sphere model, the region of solidification exists in nearly the whole particle; that is, the transitions of different phases happen throughout the particle simultaneously. The schematic diagram of this model is shown in Fig. 3. The temperature of the Al_2O_3 particle also stays constant ($T = 2310$ K) in the modeling stage. Because the solidification mode is different, the morphology of the mixture is different from the three-layered sphere.

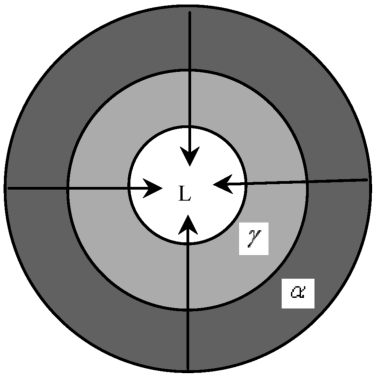

Fig. 2 Schematic diagram of multilayered sphere model.

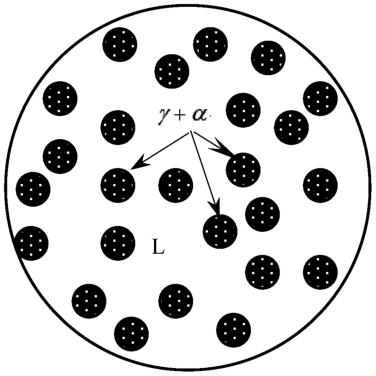

Fig. 3 Schematic diagram of effective-medium sphere model.

Then EMT is applied to calculate effective optical constants [complex refractive index $m(n, k)$ and complex dielectric constant $\varepsilon(\varepsilon', \varepsilon'')$] for this multiphase Al_2O_3 particle. In this model, several different mixing rules [12] are adopted, including the the VADC, VARI, Bruggeman mixing rule, and M–G mixing rule.

The volume-average dielectric constant and the volume-average refractive index are defined as follows:

$$\varepsilon = \sum_{x=1}^{k} \varepsilon_x F_x \tag{14}$$

$$m = \sum_{x=1}^{k} m_x F_x \tag{15}$$

The Maxwell–Garnett mixing rule is defined as

$$\frac{\varepsilon - \varepsilon_d}{\varepsilon + 2\varepsilon_d} = \sum_{x=1}^{k} F_x \frac{\varepsilon_x - \varepsilon_d}{\varepsilon_x + \varepsilon_d} \tag{16}$$

where ε_d is the dielectric constant of the host medium. In this Note, the phase state with the maximum volume fraction during the phase transition is taken as the host medium.

Table 1 Refractive index of alumina particles

Phase	Liquid	Gamma	Alpha
$\lambda = 0.35, 0.40, 0.45$, and $0.50\ \mu$m	1.744 [13]	1.65 [9]	1.78 [9]

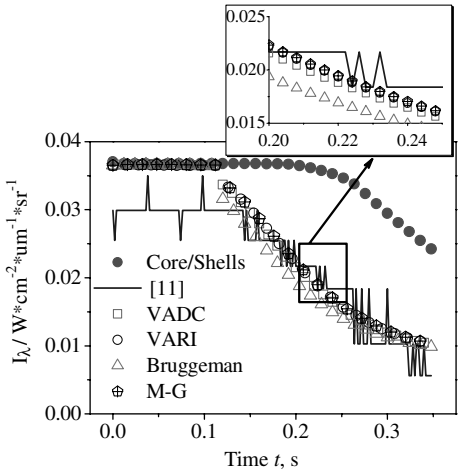

Fig. 4 Spectral radiance during the phase transition, $\lambda = 0.35\ \mu$m.

The Bruggeman mixing rule formula is expressed as

$$\sum_{x=1}^{k} F_x \frac{\varepsilon_x - \varepsilon}{\varepsilon_x + 2\varepsilon} = 0 \tag{17}$$

For the relation of refractive index and dielectric constant,

$$\varepsilon' = n^2 - k^2 \tag{18}$$

$$\varepsilon'' = 2nk \tag{19}$$

The volume fraction F_x of the x component is deduced from Eqs. (2) and (7–11); when Eqs. (14), (16), and (17) are applied, the dielectric constant of each component can be calculated by the corresponding complex refractive index. Then the time dependence of the absorption factor and the spectral radiance can be achieved by Mie theory and Eqs. (12) and (13).

IV. Results and Discussion

The spectral radiance of alumina particles with a diameter of 1.2 mm is calculated in the phase transition, and the wavelengths are chosen as 0.35, 0.40, 0.45, and 0.50 μm. The complex refractive indices at these wavelengths are shown in Tables 1 and 2 . The wavelength has little influence on the real part (refractive index) of complex refractive index, and so the refractive index in this Note is only changed with phases.

The results are shown in Figs. 4–7, in which "Core/Shells" corresponds to the results of the multilayered sphere model, and the others correspond to the results of the effective-medium sphere model with different mixing rules. It can be summarized that the present results show a trend similar to the experimental data [11]. But the results of multilayered sphere model have distinct discrepancy with the experimental results. The reason is that the solidification mode in the multilayered sphere model is too coarse. Experimentally, there are many factors influencing the crystallization process, and so there is not an exact geometry for the morphology of the experimental particle during the phase transition. The appropriate mixing rules are required for this complex morphology, and several mixing rules based on effective-medium theory are used in the effective-medium sphere model. The results of the effective-medium

Table 2 Absorption coefficient of alumina particles

Phase	Liquid	Gamma	Alpha
$\lambda = 0.35\ \mu$m	2.002034E − 3 [14]	1.05E − 4 [11]	6.28455E − 06 [14]
$\lambda = 0.40\ \mu$m	8.1079E − 4 [14]	2.38097E − 04 [14]	2.52970E − 06 [14]
$\lambda = 0.45\ \mu$m	6.30863E − 04 [14]	3.33176E − 04 [14]	2.352E − 06 [14]
$\lambda = 0.50\ \mu$m	5.92183E − 4 [14]	2.70964E − 04 [14]	1.75900E − 06 [14]

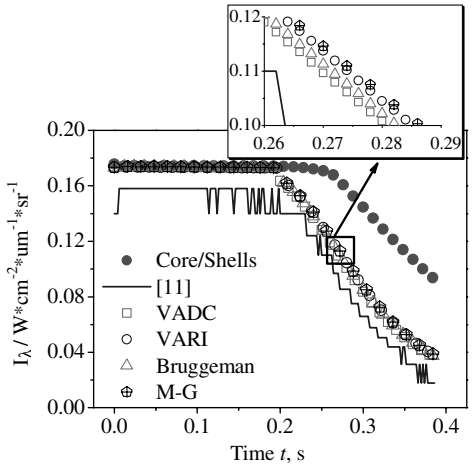

Fig. 5 Spectral radiance during the phase transition, $\lambda = 0.40$ μm.

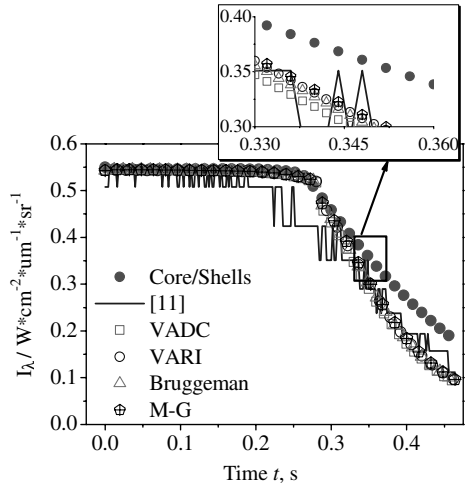

Fig. 6 Spectral radiance during the phase transition, $\lambda = 0.45$ μm.

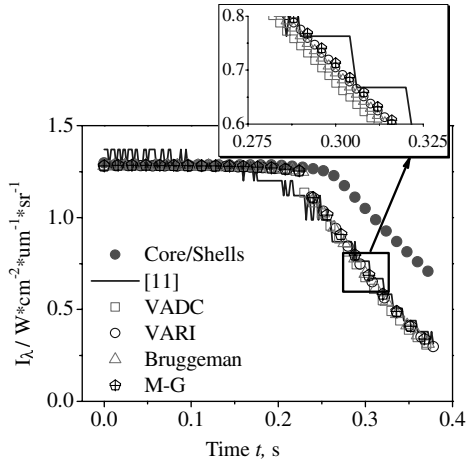

Fig. 7 Spectral radiance during the phase transition, $\lambda = 0.50$ μm.

sphere model show satisfactory agreement with the experimental data [11].

V. Conclusions

Based on the crystallization kinetic equation, two kinds of models are built up to calculate the transient spectral radiative properties of Al_2O_3 particles during phase transition, including the multilayered sphere model and the effective-medium sphere model. By comparing the present results with experimental data, it is found that more discrepancies exist between the results of the multilayered sphere model and experiment data, although the result of the effective-medium sphere model shows better agreement with the experimental data. So it is concluded that the morphology of the mixture should be considered in the modeling of transient radiative properties of Al_2O_3 particles with phase transition.

Acknowledgments

This work was supported by International Cooperation Item of National Natural Science Foundation of China (grant no. 50620120442) and National Natural Science Foundation of China (grants no. 50506009). The authors also thank L. H. Liu for his useful suggestion.

References

[1] Zhou, H. C., Ai, Y. H., "Effect of Radiative Transfer of Heat Released from Combustion Reaction on Temperature Distribution: A Numerical Study for a 2-D System," *Journal of Quantitative Spectroscopy and Radiative Transfer*, Vol. 101, No. 1, 2006, pp. 109–118. doi:10.1016/j.jqsrt.2005.11.008

[2] Zhou, H. C., Han, S. D., Sheng, F., and Zheng, C. G., "Visualization of Three-Dimensional Temperature Distributions a Large-Scale Furnace via Regularized Reconstruction from Radiative Energy Images: Numerical Studies," *Journal of Quantitative Spectroscopy and Radiative Transfer*, Vol. 72, No. 4, 2002, pp. 361–383. doi:10.1016/S0022-4073(01)00130-3

[3] Plastinin, Y. A., Anfimov, N. A., Baula, G. G., Karabadzhak, G. F., Khmelinin, B. A., and Rodionov, A. V., "Modeling of Aluminum Oxide Particle Radiation in a Solid Propellant Motor Exhaust," AIAA Paper 1996-1879, 1996.

[4] Rodionov, A. V., Plastinin, Y. A., Drakes, J. A., Simmons, M. A., and Hiers, R. S., "Modeling of Multiphase Alumina-Loaded Jet Flow Fields," AIAA Paper 1998-3462, 1998.

[5] Gossé, S., Sarou-Kanian, V., Véron, E., Millot, F., Rifflet, J. C., and Simon, P., "Characterization and Morphology of Alumina Particles in Solid Propellant Subscale Rocket Motor Plumes," AIAA Paper 2003-3649, 2003.

[6] Burt, J. M., and Boyd, I. D., "A Monte Carlo Radiation Model for Simulating Rarefied Multiphase Plume Flows," AIAA Paper 2005-4691, 2005.

[7] Gosśe, S., Hespel, L., Gossart, P., and Delfour, A., "Morphological Characterization and Particle Sizing of Alumina Particles in Solid Rocket Motor," *Journal of Propulsion and Power*, Vol. 22, No. 1, 2006, pp. 127–135.

[8] Voshchinnikov, N. V., and Mathis, J. S., "Calculating Cross Sections of Composite Interstellar Grains," *Astrophysical Journal*, Vol. 526, No. 1, 1999, pp. 257–264. doi:10.1086/307997

[9] Oliver, S. M., and Moylan, B. E., "An Analytical Approach for the Prediction of Gamma-to-Alpha Phase Transformation of Aluminum Oxide (Al_2O_3) Particles in the Space Shuttle ASRM and RSRM Exhausts," AIAA Paper 1992-2915, 1992.

[10] Plastinin, Y. A., Sipatchev, H. P., Karabadzhak, G. F., Khmelinin, B. A., Szhenov, E. Y., Khlebnikov, A. G., and Shishkin, Y. N., "Experimental Investigation of Alumina Particles' Phase Transition and Radiation," AIAA Paper 1998-0862, 1998.

[11] Plastinin, Y. A., Afanasjev, A., Sipatchev, H., Szhenov, E., Khlebnikov, A., Khmelinin, B., Shishkin, Y., and Shesterkin, I., "Experimental Investigation of Alumina Particles' Phase Transitions," European Office of Aerospace Research and Development, Rept. SPC-95-4023, FPO New York, NY, Dec. 1995.

[12] Choy, T. C., *Effective Medium Theory: Principles and Applications*, Oxford Univ. Press, Oxford, 1999, pp. 7–15.

[13] Krishnan, S., Weber, J. K. R., Schiffman, R. A., Nordine, P. C., and Reed, R. A., "Refractive Index of Liquid Aluminum Oxide at 0.6328 μm," *Journal of the American Ceramic Society*, Vol. 74, No. 4, 1991, pp. 881–883. doi:10.1111/j.1151-2916.1991.tb06947.x

[14] Plastinin, Y. A., Karabadzhak, G. F., Khmelinin, B. A., Baula, G., and Rodionov, A., "Ultraviolet, Visible and Infrared Spectra Modeling for Solid and Liquid-Fuel Rocket Exhausts," AIAA Paper 2001-0660, 2001.